Supporting Information

Rahimi et al. 10.1073/pnas.1422785112

SI Text

Experimental

The preparation of liquid crystal (LC)-in-water emulsions and the adsorption of polystyrene (PS) particles onto the surface of LC droplets have been described in detail before (1). Here, we only provide a brief account of the systems considered here. Nematic droplets were prepared by emulsifying 4 μL of 5CB in 1.98 mL of an aqueous phase. The emulsification was performed in a T25 digital ULTRA-TURRAX homogenizer equipped with an S25 N-10G dispersing element. To adsorb PS particles onto the surfaces of the LC droplets, 20 μL of 1% (wt/vol) PS particles were added to the 1.98 mL of the LC-in-water emulsion. The mixture was then homogenized at 6,400 rpm. The duration of homogenization was 30, 45, 60, or 300 s for adsorption of two, three and four, five, six and seven, or more PS particles, respectively.

To characterize assemblies of particles at the surface of a droplet, fluorescently labeled PS colloids (λ_{exc} = 480 nm/λ_{em} = 520 nm) were used. To capture micrographs, a 50-μL aliquot of the LC emulsion was dispensed onto a glass coverslip. The LC droplets were then imaged using an Olympus IX71 inverted epifluorescence microscope equipped with a 100× oil- immersion objective, crossed polarizers, mercury lamp, and Chroma filter (457 nm ≤ λ_{exc} ≤ 502 nm, and 510 nm ≤ λ_{em} ≤ 562 nm). Fluomicrographs of LC-in-water emulsions were collected with a Hamamatsu 1394 ORCAER CCD camera connected to a computer and controlled through SimplePCI imaging software (Compix).

Using fluomicrographs, the diameter of PS particles and the center-to-center distance between PS particles were measured to be 1.01 ± 0.01 and 1.17 ± 0.06 μm, respectively. The error represents the SD over 30 fluomicrographs. That measurement indicates that the PS particles are not closely packed.

The depth to which particles submerge into the droplets was measured to determine the contact angle between the droplet surface and the particle surface. As shown in the Fig. S1, for a PS particle of 4-μm diameter, the contact angle at the surface of the nematic 5CB LC droplet was found to be 95°, which confirms that one-half of the particle is inside the droplet (2).

Simulation

The tensor representation of the LC is based on a spatial average of the dyadic product of individual molecular orientations (3, 4). The order parameter Q tensor is defined as follows:

$$Q = <nn - \frac{1}{3}\delta>,$$

where n is a vector aligned with the long axis of each molecule, and δ is the Kronecker delta. According to this definition, Q is a traceless tensor. The Q tensor can be diagonalized and written as follows:

$$Q = \begin{pmatrix} \frac{2S}{3} & 0 & 0 \\ 0 & \frac{\mu - S}{3} & 0 \\ 0 & 0 & \frac{-\mu - S}{3} \end{pmatrix},$$

where the S is the scalar order parameter and μ is biaxial order.

The free energy of the system is defined as a function of the Q tensor and includes three contributions: the short-range Landau–de Gennes, long-range elastic, and surface free-energy densities. A general free-energy expression is written as follows:

$$F(Q) = \int_V (f_{LdF}(Q) + f_E(Q))dV + \int_S (f_s(Q))ds.$$

The short-range Landau–de Gennes, long-range elastic, and surface free-energy densities are given as f_{LdF}, f_E, and f_s, respectively. The short-range free energy is represented by a Landau–de Gennes expression of the following form (3):

$$f_{LdF}(Q) = \frac{A}{2}\left(1 - \frac{U}{3}\right)Q_{ij}Q_{ji} - \frac{AU}{3}Q_{ij}Q_{jk}Q_{ki} + \frac{AU}{4}(Q_{ij}Q_{ji})^2,$$

where A and U are material parameters that capture the thermodynamics of the LC. These parameters set an energy scale for the phase transitions A, and bulk scalar order parameter U.

For a uniaxial system, the elastic contribution to the free energy to second order is written as follows (3, 4):

$$f_E = \frac{L_1}{2}\frac{\partial Q_{ij}}{\partial x_k}\frac{\partial Q_{ij}}{\partial x_k} + \frac{L_2}{2}\frac{\partial Q_{jk}}{\partial x_k}\frac{\partial Q_{ji}}{\partial x_i} + \frac{L_4}{2}\frac{\partial Q_{jk}}{\partial x_i}\frac{\partial Q_{ji}}{\partial x_k}.$$

The L constants are associated with different spatial deformations, and they can be mapped onto the director elastic constants (5). These mappings are as follows:

$$L_1 = \frac{k_{33} - k_{11} + 3k_{22}}{6S^2}, \quad L_2 = \frac{k_{11} - k_{22} - k_{24}}{S^2}, \quad L_4 = \frac{k_{24}}{S^2}.$$

The k constants describe the independent modes of deformation in director representation, namely: splay (k_{11}), twist (k_{22}), bend (k_{33}) and saddle-splay (k_{24}). The single elastic constant approximation, where $k_{11} = k_{22} = k_{33} = k_{24}$, is widely used in the literature and was adopted in this work (6–9).

The final term in the free energy describes the interaction of the LCs with the surfaces. Depending on the anchoring type, there are different forms that define the surface potential. Here, we restrict our attention to degenerate planar anchoring, which is described by a Fournier and Galatola expression of the following form (10):

$$f_s = w\left(\tilde{Q} - \tilde{Q}^{\perp}\right)^2,$$

where

$$\tilde{Q} = Q + \frac{S}{3}\delta, \quad \tilde{Q}^{\perp} = P.\tilde{Q}.P, \quad P = \delta - \nu\nu.$$

The projection of the tensor on the surface is defined by $\tilde{Q}^{\perp}$, ν is the normal vector at the surface, and w denotes the strength of the surface anchoring.

The total free energy is minimized by using the Euler–Lagrange algorithm (4). Equilibrium conditions for bulk and surface are given as follows:

$$\frac{\partial f}{\partial Q} - \nabla\frac{\partial f}{\partial \nabla Q} = 0 \text{ (bulk)}, \quad \frac{\partial f}{\partial \nabla Q}.\nu = 0 \text{ (surface)}.$$

Again, here ν represents the surface normal.

Our systems exhibit both surface and bulk contributions to the free energy, and, therefore, the nodes on the surface of the droplet and particles must be identified. To define bulk and surface nodes for the droplet, we select all nodes located inside a sphere with radius $R_d + \Delta X/2$, where R_d is the radius of droplet and ΔX is the grid resolution. All nodes with six neighbors in the sphere are considered to be bulk nodes, and the remaining nodes (with at least one bulk neighbor) are defined as the surface nodes. The center of each particle is located at a distance R_d from the center of the droplet, and the method just described for assigning surface and bulk nodes is also used to define the particle surface nodes. All simulations were begun from a uniform director field, with the nematic director aligned with the z axis. Such an initial condition encourages two boojums to arise exactly at the z axis after relaxation, even in the presence of particles. This allows for the systematic study of free energy as a function of the angle (or distance) between the two polar boojums and the location of the adsorbed particles.

All of our original calculations assumed that one-half of the volume of each particle is inside the droplet. To assess the effect of the depth that particles submerge into the droplet in our results, we repeated our calculations assuming that 40% or 60% of the particle volume was inside the droplet. We found that changing the depth does not substantially affect to the interaction between particles or the interaction between particles and the boojum. A representative set of results is shown in Fig. S2, where we present the free energy of a particle as a function of its angle with the boojum for three different depths. One can see that the overall shapes of the corresponding free-energy profiles are similar, indicating that small changes of contact angle in the neighborhood of 95° are not sufficient to alter the conclusions of our work. Note that, for the system with 60% of the particle inside the droplet, the free energy close to the boojum is deepest, because the particle can occupy a larger volume with a high elastic energy at the pole.

1. Mondiot F, Wang X, de Pablo JJ, Abbott NL (2013) Liquid crystal-based emulsions for synthesis of spherical and non-spherical particles with chemical patches. *J Am Chem Soc* 135(27):9972–9975.
2. Wang X, Miller DS, de Pablo JJ, Abbott NL (2014) Organized assemblies of colloids formed at the poles of micrometer-sized droplets of liquid crystal. *Soft Matter* 10(44): 8821–8828.
3. De Gennes P, Prost J (1995) *The Physics of Liquid Crystals* (Oxford Univ Press, Oxford).
4. Ravnik M, Žumer S (2009) Landau–de Gennes modelling of nematic liquid crystal colloids. *Liq Cryst* 36(10-11):1201–1214.
5. Mori H, Gartland EC, Kelly JR, Bos PJ (1999) Multidimensional director modeling using the Q tensor representation in a liquid crystal cell and its application to the π cell with patterned electrodes. *Jpn J Appl Phys* 38(Pt 1, No 1A):135–146.
6. Nych A, et al. (2013) Assembly and control of 3D nematic dipolar colloidal crystals. *Nat Commun* 4:1489.
7. Musevic I, Skarabot M, Tkalec U, Ravnik M, Zumer S (2006) Two-dimensional nematic colloidal crystals self-assembled by topological defects. *Science* 313(5789):954–958.
8. Ravnik M, et al. (2007) Entangled nematic colloidal dimers and wires. *Phys Rev Lett* 99(24):247801.
9. Ravnik M (2009) Nematic colloids entangled by topological defects. *Soft Matter* 5(2): 269–274.
10. Fournier J-B, Galatola P (2005) Modeling planar degenerate wetting and anchoring in nematic liquid crystals. *Europhys Lett* 72(3):403–409.

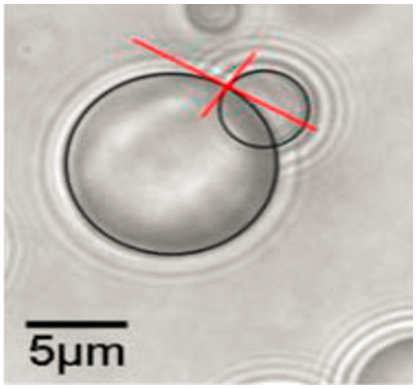

Fig. S1. A 4-μm-diameter PS particle adsorbed at the surface of nematic LC droplet. The contact angle was measured to be ~95°. Reproduced from ref. 2 with permission of The Royal Society of Chemistry (dx.doi.org/10.1039/C4SM01784F).

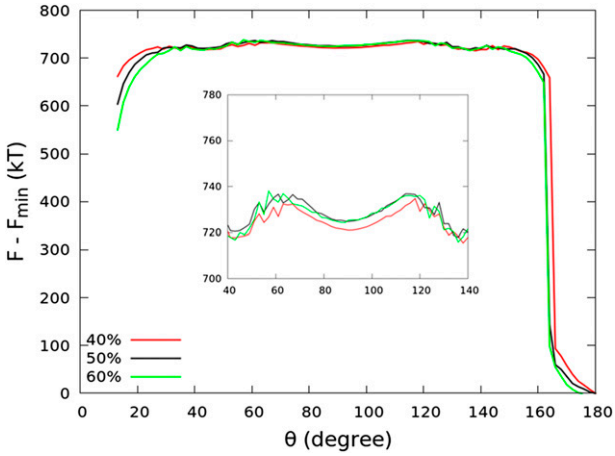

Fig. S2. The free energy of a particle as a function of polar angle θ for three different depths. One particle is located at the boojum along the *z* axis, and the other is driven along the droplet surface.